ICCRR
6th International Conference on Concrete Repair, Rehabilitation and Retrofitting
CAPE TOWN 03 – 05 OCTOBER 2022

Ion distribution in concrete overlay, mapped by laser induced breakdown spectroscopy (LIBS), modified by an embedded zinc anode

W. Schwarz[1)], Gerd Wilsch[2)], N. Katsumi[1)], G. Ebell[2)], T. Völker[2)]

[1]CAS Composite Anode Systems GmbH, Vienna, Austria
[2]Bundesanstalt für Materialforschung und -prüfung, Berlin, Germany (BAM)

Abstract.. Galvanic corrosion protection by embedded zinc anodes is an accepted technique for the corrosion protection of reinforcing steel in concrete. Galvanic currents flow between the zinc anode and the steel reinforcement due to the potential difference that is in the range of a few hundred mV. The ion distribution was studied on two steel reinforced concrete specimens admixed with 3 wt.% chloride/wt. cement and galvanically protected by a surface applied EZ-anode. On both specimens, a zinc anode was embedded and glued to the concrete surface by a geo-polymer-based chloride-free binder. At one specimen, the EZ-anode was operated for 2,5 years, the EZ-anode at the other specimen was not electrically connected to the reinforcement, this specimen serves as a reference. Both specimens have been stored under identical conditions. The ion distribution between the anode (EZ-anode) and cathode (steel reinforcement) was studied by laser-induced breakdown spectroscopy (LIBS) after 7 months, 12 months, and 2,5 years. Results of the LIBS studies on the specimen with activated EZ-anode after 7 months, 12 months, and 2,5 years and of the reference specimen after 2,5 years are reported. Results show that diffusion of ions contributes to the changes in the ion distribution but migration, especially of chlorides towards the EZ-anode is significant despite the weak electric field – several hundred millivolts - generated by the galvanic current. Results show that chloride ions accumulate near the zinc-anode as in water-insoluble zinc-hydroxy chlorides - Simonkolleit.

1 Introduction

Galvanic corrosion protection of steel in concrete is based on the formation of a galvanic element. This requires a metal that has a more negative free corrosion potential than the reinforcement and an electrical connection between them, and also an electrolytic connection. The reinforcing steel is protected from corrosion as long as sufficient galvanic current flows between the galvanic anode and the steel reinforcement. Most commonly, zinc is used as the sacrificial anode material. The galvanic element formed corresponds to a conventional zinc/air battery that is becoming popular again as an alternative source of energy.

Galvanic corrosion protection was first employed to protect a bridge deck in Illinois in 1977 within the cooperative highway research program, with mixed results [1]. A problem with the initially applied sacrificial anodes was, that their protection current decreases with time, and they eventually become passive. Due to this, most systems have a relatively short useful life [2].

In the 1990's, sacrificial anode systems based on sprayed zinc anodes, zinc foil glued to the concrete surface (zinc hydrogel system), and zinc mesh pile jackets around bridge columns filled with sea water were starting to be evaluated and used for the protection of bridge structures [2 – 5].

The efficiency of galvanic corrosion protection depends on the lasting activity of the zinc anode. Deposition and agglomeration of the zinc-based corrosion products like zinc hydroxide and zinc hydroxy chlorides or contact with calcium hydroxide in the pore solution may passivate the zinc anode surface. The service time of the zinc anode may be limited by self-corrosion which increases with the activation of the zinc anode and may reach up to 70% of the zinc consumed during operation.

A galvanic zinc anode system composed of a zinc mesh embedded into a proprietary mortar that solidifies into a solid electrolyte, installed on various civil structures (bridges, marine harbor piles, parking decks, tunnel entrances) could protect the steel reinforcement reliably and efficiently from corrosion for at least 11 years [6]. The solid electrolyte of the embedded zinc anode system (EZ-anode) is based on a tecto-alumosilicate-binder (TAS) containing additives that prevent passivation of the zinc anode, assure high and durable galvanic activity of the zinc anode, and high and durable adhesion towards the concrete overlay.

Previous studies of concrete overlay samples drawn from field installations indicated chloride migration and chloride fixation near the zinc anode [7], however verification and quantification on samples drawn from field installations proved to be difficult as the original chloride distribution in the concrete and the embedding mortar are difficult to evaluate.

* Corresponding author: schwarz@cas-composite.com

Migration of chlorides in concrete in an applied electric field is well established and employed e.g. for rapid determination of diffusion constants in concrete [8-10]. The electric field generated by the galvanic current, is estimated to be in the range of 300 – 600 mV, estimated from the open-circuit potential between zinc-anode and steel reinforcement, and is much lower than the electric fields usually applied (about 1 Ampere /m^2) for electrochemical chloride extraction [11] or for cathodic protection of steel in concrete [12]. Migration is only slightly influenced by the applied electric field at high electric fields (e.g. 5 – 10 Volts, about 1 Ampere/m^2) and is mainly controlled by the current [13]. The influence of the electric field on migration at very low field strength is not well studied. The transport of chlorides in concrete is controlled by migration and by diffusion. As outlined before [14,15], chlorides are immobilized near the zinc-anode as water-insoluble zinc-hydroxo-chlorides (Simonkolleit). This should lead to a high concentration gradient inducing chloride diffusion towards the zinc-anode.

Therefore, the performance of an EZ-anode embedded into a chloride-free embedding TAS binder (shrinkage reduced embedding zinc activating cement – SEZAC) was studied and evaluated under controlled laboratory conditions on two concrete specimens equipped with a zinc anode embedded and glued to the concrete surface by a geo-polymer-based chloride free binder. On one specimen, the EZ-anode was operated over a period of 2,5 years by connecting it to the steel reinforcement, the EZ-anode of the other specimen was not activated. Both specimens have been stored under identical conditions. The influence of the galvanic field on the ion distribution in comparison to the reference sample in which only diffusion is the driving force for ion transport, especially on the chloride transport in the concrete overlay and the embedding binder could be evaluated and visualized by LIBS – laser-induced breakdown spectroscopy. Results are reported in this paper; evaluations by REM and EDX are under way and will be reported soon in CCR (Cement and Concrete Research).

2. Experimental

2.1. Galvanic Anode/Mortar Probe

Table 1: steel reinforced mortar - test plates

dimensions	28 x 21 x 6 cm	
steel reinforce-ment	Ø 10 mm spacing: e 17 connecting steel	4 bars à 240 mm 4 mm & 6 mm
mortar	SikaMonotop 412 N water sodium chloride	13,85 kg 2,0 kg 0,242 kg 0,84 wt.% Cl/kg fresh mortar
reference cell	ERE 20	Type: Mn/MnO_2

Note: SikaMonotop 412 N mortar was chosen as being certified for CP use. The cement content is rather high (640 kg/m^3 fresh mortar).
Embedding binder for zinc mesh: geopolymer based 2-component SEZAC binder admixed with ground marble filler. Mixing ratio component A (binder), component B (aqueous high alkali potassium silicate), Filler (0,2 – 0,5 mm ground marble):
A : B : Filler = 100:50:104
Specific weight of wet binder: 1,84 kg/liter
Zinc-mesh: 99% zinc alloy, mesh size 5 mm – 7 mm, wire diameter 1,1 mm; 2,7 kg zinc/m^2 mortar surface, 1,1 kg zinc-mesh per plate embedded into 0,750 kg SEZAC binder.
The EZ-anode probes were stored at 99% rh at RT for 1 week for initial hardening and then stored at 80% rh for an additional week.

2.2. Operation of the EZ-Anode Galvanic Anode System

The EZ-anode probes were stored in a climatized compartment at 75% rh. Current between the steel reinforcement and the zinc anode was measured over a 0,1 Ohm shunt and transformed into voltage with an operational amplifier. Steel potentials were measured with a 20 MΩ input impedance. Data were recorded by a MODAC data logger. Additionally, steel potentials were measured manually with an Ag/AgCl reference cell placed onto the surface of the mortar probe.

2.3. Laser Induced Breakdown Spectroscopy (LIBS)

The LIBS technique was used for the investigation of the ion transport processes. LIBS - is a combination of laser ablation and plasma generation by a short (ns) high energy (several mJ) laser pulse and the analysis of the emitted radiation by optical spectroscopy. LIBS can capture all elements of the periodic table simultaneously through the underlying measurement principle [16]. An overview of the potential of LIBS for the investigation of building materials can be found in the literature [15-20]. For the investigation in this paper, the FiberLIBSlab system from SECOPTA analytics was used (see fig. 1).

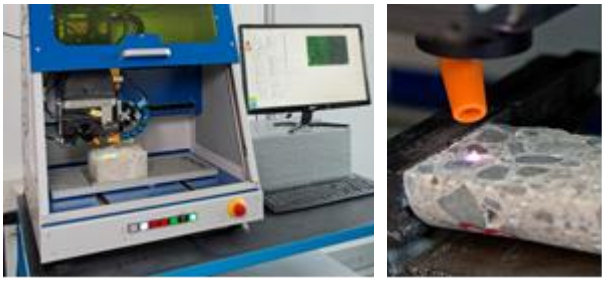

Fig. 1. Overall view of the LIBS laboratory system (left). Detailed view on the sample surface with plasma and nozzle of helium feeder (right).

For the quantitative analysis, a calibration of the system with 15 reference samples based on cement (CEM I) with a concentration range of chloride of 0,05 to 2,5 wt% was performed. The limit of detection for chlorine in concrete is 0,04 % regarding the mass of cement. A scanner is used to obtain a two-dimensional element mapping.

Table 2: main parameters of the used LIBS system

Plasma generation	Detection of radiation
NdCr:YAG-laser: 1064 nm, 3 mJ, 1.5 ns, 100 Hz passive Q-switch	spectrometer: Czerny-Turner 1200 lines/mm, 2048 pixel temperature stabilised
Ø laser spot: 80 µm	NIR 750 nm - 950 nm UV 230 nm - 500 nm
power density: 40 GW/cm²	elements: NIR: Ca, O, K, Na, Cl, C, S UV: Ca, Si, Mg, Al, Fe, Ag, Ti
process gas:	helium
integrated scanner:	$A_{max.}$ = 14 cm x 17 cm

All the elements listed in table 2 were recorded simultaneously for each measuring point. The multielement information can be used for exclusion of aggregates, rebars or points belonging to the zinc anode by defining limits for the LIBS-signals in the software.

The galvanic anode/mortar probes were cut along the broad side for performing the LIBS measurements on the cross-section as shown in fig. 2:

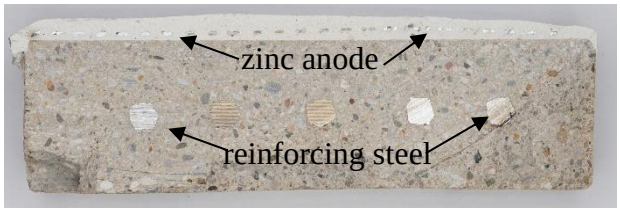

Fig. 2a. EZ-anode/mortar probe, galvanically active for 2,5 years, cut broadside for LIBS measurements

Fig. 2b. EZ-anode/mortar reference probe, stored for 2,5 years under the identical conditions as the galvanic active probe, cut broadside for LIBS measurements

The galvanically active probe shows no cracks and no corrosion on the steel reinforcement (fig. 2a), the galvanically not activated reference probe shows cracks due to voluminous corrosion products at the steel surface (fig. 2b).

On the sample an area of about 85 mm by 65 mm measurements were taken with a spatial resolution of 0.5 mm x 0,5 mm. As result, the element distribution was plotted as a multicolor image over the measured area (e.g. fig. 4). Three samples were prepared after 7 months, 12 months, and 2,5 years of galvanic operation. Samples were taken from the reference probe after 2,5 years.

3. Results

3.1. Galvanic Performance

The galvanic current between the EZ-anode mounted on the mortar probe stored in a climatized chamber (75% rh, 20 – 25°C) and the steel reinforcement was monitored. The current flow over 2,5 years' time is shown in fig. 3.

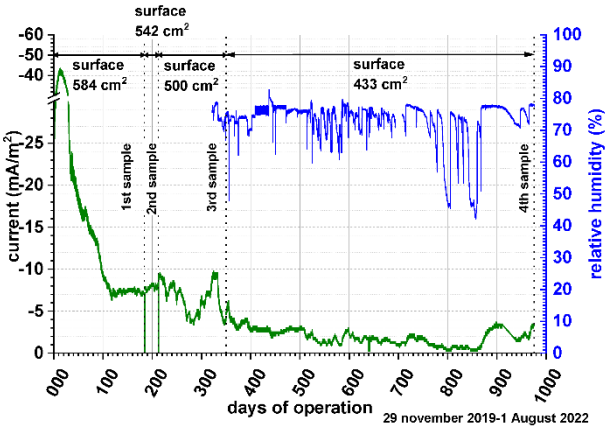

Fig. 3. Galvanic current flow over time at 75% rh and room temperature.

The galvanic current stabilized after about 8 months of operation at 5 mA/m^2 and about 3,5 mA/m^2 after 2,5 years at 75% rh. The galvanic current proved to be sensitive to the ambient relative humidity as shown in fig 3: Relative humidity's of 45% to 55% resulted in a quickly reversible reduction of the galvanic currents to about 1 mA/m^2. The galvanic operation resulted in a significant shift of the steel potentials toward positive values (operational data are summarized in table 3). 24 h depolarisation according to EN 12696 after 12 months of operation yielded a value of 138 mV.

Table 3. steel potentials before and during galvanic operation of EZ-anode mounted on the mortar probe during 24 h depolarisation measurements (off-potentials)

Time of galvanic operation [month]	0	7	12	32,5
24 h off-potential [mV]	-374	-246	-172	*
Charge passed [kC]	**0**	247	344	450

*Reference cell was cut after 12 month of operation (fig. 5)

After 32,5 months of operation, no visible corrosion of the zinc anode could be detected (fig. 2a) but significant corrosion in the non-protected reference sample (fig. 2b).

3.2. LIBS measurements

LIBS measurements were performed on samples cut after 5, 7, 12 months and 2,5 years of galvanic operation of EZ-anode mounted on the mortar probe.

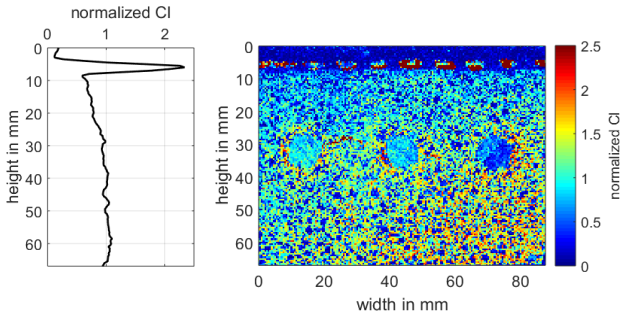

Fig. 4. Colour coded chlorine distribution determined by LIBS in the cross section of EZ-anode/mortar probe after 7 months of galvanic operation (right) and depth profile of chlorine (left). The chloride content is normalized to the chloride content of the mortar in areas not exposed to the electric field generated by the galvanic current.

After 7 months of operation, chloride migration towards the anode was significant, creating a depletion zone (that was not yet visible after 5 month of galvanic operation) between the steel reinforcement and the zinc-anode. The chloride accumulated near the zinc-anode – there was no chloride in the binder material itself detectable (fig. 4) and the chloride gradient between steel reinforcement (cathode) and anode increased significantly after 5 months additional, total 12-month galvanic operation (fig. 5).

Note: the circular area with an apparent red circle in it (o), between the two rebars on the left side, originates from a cut Ag/AgCl reference cell, the red circle is due to the KCl electrolyte.

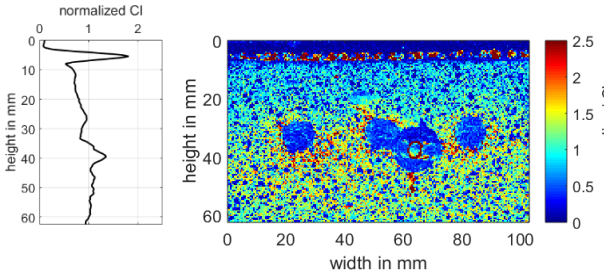

Fig. 5. Colour coded chlorine distribution determined by LIBS in the cross section of EZ-anode/mortar probe after 12 months of galvanic operation (right) and depth profile of chlorine (left).

After 2,5 years of galvanic operation, the chloride accumulation at the EZ-anode and the gradient between the cathodic steel reinforcement and the EZ-anode increases significantly (fig. 6): the chloride concentration at the interface EZ-anode binder/concrete is reduced from 1,2 wt.% to 0,67 wt. % and the chloride concentration in the binder layer encompassing the zinc-anodes increases to about 2,5 wt. %. The concentration in the binder matrix between EZ-anode and concrete interface is about 0,1 wt.%. The concentration around the zinc-anode reaches values of 13,8 wt. %. The chloride concentration near the steel reinforcement is reduced from 1,2 wt.% to 0,8 wt.%. Therefore, after 2,5 years of galvanic operation, there is a significant transport of chloride ions towards the EZ-anode and a slight reduction of the chloride concentration near the steel cathode.

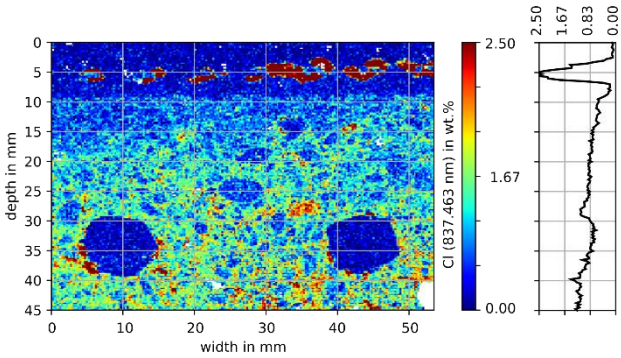

Fig. 6. Chloride distribution determined by LIBS in the cross section EZ-anode/mortar probe after 2,5 years of galvanic operation

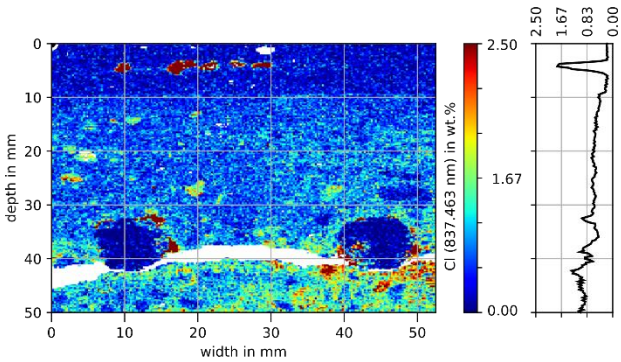

Fig. 7. Chloride distribution in the galvanically non activated EZ-anode/mortar reference sample, determined by LIBS in the cross section after 2,5 years.

The changes in the ion distribution in the galvanically operated sample are due to migration and diffusion. A reference sample – identical with the galvanically operated sample, but galvanically not active (the EZ-anode was not connected to the steel reinforcement) was stored in the same climatized chamber to estimate the contribution of diffusion. The distribution of chloride after storage of 2,5 years is shown in fig. 7:

Chloride accumulates around five out of thirteen of the embedded zinc-metal parts – left side in fig. 7 - and around the steel reinforcement bars. The amount of chloride accumulated around the zinc-metal parts is about 50% of the amount observed around the EZ-anode parts in the galvanically operated sample (fig. 6). As the LIBS iron scan shows, the chloride accumulated around the steel rebars is present as iron(III)chloride due to severe corrosion of the steel rebars – leading to the cracking of the concrete matrix – the white broad line in fig. 7. A weak chloride gradient is observed in the concrete cover towards the interface EZ-anode-binder/concrete. As there is no electric field generated between the embedded zinc mesh and the steel reinforcement – transport of chloride may only be due to diffusion or capillary transport due to changes in ambient humidity. Capillary transport is

assumed to be negligible as the chloride concentration near the surface of the embedding binder is 0.
Chloride accumulation near the zinc-metal parts of the embedded zinc-mesh in the reference sample (fig. 7) is nearly identical with chloride accumulation in the galvanically operated sample (13,8 vs. 14 wt.%): LIBS data show that chloride occurs only together with zinc therefore (see chapter 2.3.) - it is assumed to be present as Simonkolleit:
The software of the LIBS allows, as described in chapter 2.3., the exclusion of the areas that contain zinc, iron and aggregate as shown in fig. 8 & 9: In the area of Zn-exclusion, chloride concentration is nearly zero – indicating that the chloride was linked to anodic zinc products accumulated in the vicinity of the zinc-anode.

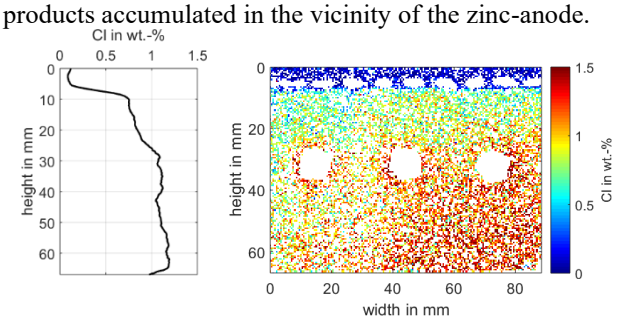

Fig. 8. Chloride distribution determined by LIBS in the cross section EZ-anode/mortar probe after 7 months of galvanic operation: Zn, Fe & aggregate excluded/deducted (white).

The given quantitative chloride values (fig. 8, 9) should only be regarded as guide values. As already mentioned, the LIBS system was calibrated with cement-based reference samples (CEM I). A deviation from the material can lead to errors in quantification due to matrix effects (e.g. here the binder).

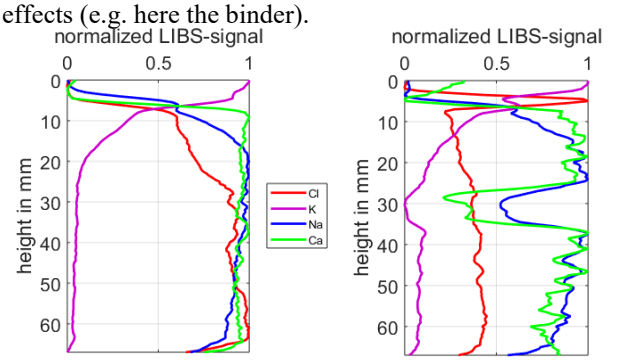

Fig. 9. Ion distribution determined by LIBS in the cross section EZ-ANODE/mortar probe after 7 months of galvanic operation: Zn, Fe & aggregate excluded/deducted (left graph) in comparison with the ion distribution without exclusion (right graph).

The distribution of chloride, potassium, sodium and calcium under the exclusion of aggregate, iron and zinc in the cross-section of the EZ-anode-mortar probe is shown in fig. 9: The chloride depletion zone is clearly visible (left graph in fig. 9). Sodium and potassium migrate towards the cathode – the binder is rich in potassium, free in sodium and nearly calcium-free – calcium is detected only in the mortar phase and in the aggregates in the binder phase (fig. 7, ion distribution without exclusion). The absence of calcium in the binder is essential for the functioning of the SEZAC binder as zinc-activating cement.
Results indicate strongly that Simonkolleit is formed only by direct reaction of the anodically dissolved zinc ions with chloride near the anode interface. Due to the anodic reactions, the solution near the anodic interface, especially the double layer, will be at least slightly anodic and zinc-chloride may be stable and will react subsequently to form Simonkolleit [21].
Therefore, the formation of Simonkolleit near the zinc mesh metal parts in fig. 7 indicates anodic polarization that may arise from auto corrosion of the zinc-mesh, the chloride free zinc mesh metal parts forming the cathode.
The solubility of Simonkolleit in alkaline aqueous media is near zero – therefore the formation of Simonkolleit creates a strong concentration from the chloride containing concrete cover towards the anodically polarized zinc-metal parts. Comparing the chloride concentrations around the zinc-metal parts of the galvanically operated sample with the reference sample, median values 3,5 wt.% vs. 1.8 wt.%, one may estimate that at least 50% of the chloride transport towards the anodically polarized zinc-mesh occurs by diffusion due to the concentration gradient created by the formation of Simonkolleit.
The very low concentration of chlorides in the zinc-embedding binder matrix may be a result of rapid diffusion due to its high porosity (about 35 vol.%) and the negative surface charge of the binder matrix, opposite to the positive surface charge of hardened cement [22].
The effects of migration and diffusion on ion diffusion is exemplified by comparing the distribution of potassium ions in the binder matrix and in the concrete cover in the galvanically active with the inactive reference sample (fig. 10 & 11):

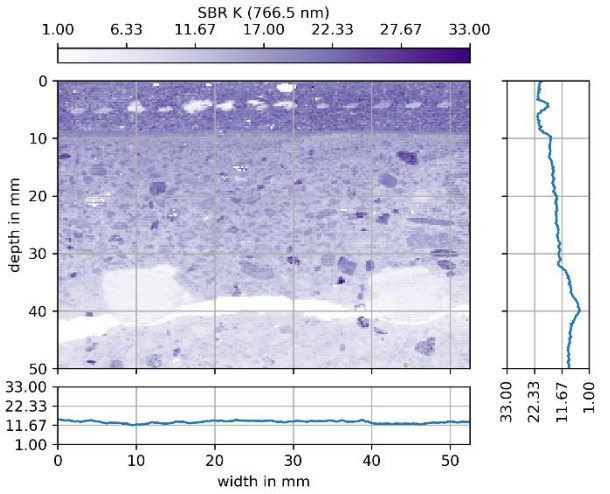

Fig. 10. Potassium ion distribution in the galvanically non activated reference sample, determined by LIBS.

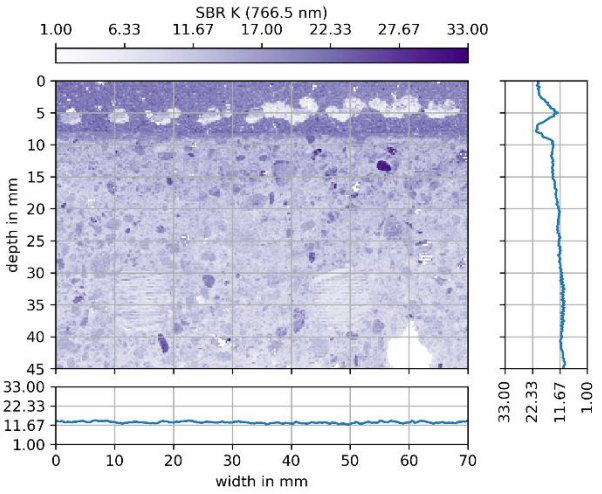

Fig. 11. Potassium ion distribution in the galvanically activated sample, determined by LIBS after 2,5 years.

The zinc embedding binder matrix contains about 4 wt.% potassium that creates a large concentration gradient towards the concrete cover (K 0,1 wt.%). Therefore, potassium ions will either diffuse (fig. 10) or diffuse and migrate (fig. 11) into the concrete cover due to the large concentration gradient or concentration gradient + electric field.

In the reference sample (fig. 10), potassium diffuses into the concrete cover leading to increasing potassium concentration in the concrete cover. Diffusion stops at the corrosion-initiated crack. A potassium depletion halo is observed around the anodically polarized zinc-mesh parts whereas no reduction in potassium concentration around the presumably cathodically polarized zinc-mesh parts is observed.

Large potassium deficient halos are observed around the anodically polarized zinc-mesh parts in the galvanically operated sample (fig. 11) as positively charged potassium ions will be repelled from the positively charged anodically polarized zinc-mesh parts. Different to the reference sample, no reduction of the potassium content due to the presence of the steel bares is visible – indicating an accumulation of potassium near the cathodically polarized steel bars, as the negatively charged steel bars will attract the positively charged potassium ions.

Therefore, results show that during the galvanic operation of the EZ-anode, applied on chloride contaminated concrete, diffusion and migration contribute both to the chloride ion transport towards the embedded zinc-mesh anode, which is at least 50% due to diffusion. Diffusion and migration act in the same direction, pulling the chloride ions towards the embedded zinc-anode. Opposite to cathodic protection systems operated with incipient current, in which chlorides accumulates near the anode due to migration, creating a concentration gradient of chloride from the anode towards the concrete - chloride ion transport towards the anode will stop if migration and diffusion balance each other out.

4. Summary and outlook

The evaluation of elemental distribution in the concrete/binder matrix by LIBS allows the investigation and graphical representation of the changes in the ion distribution caused by the applied electric field and by diffusion.

The results show that there is a significant accumulation of chloride in the vicinity of the zinc-anode directly linked to the local presence of zinc compounds resulting from the anodic reaction of zinc. Results indicate strongly that chlorides are bound and immobilized near the zinc-anode as in water insoluble Simonkolleit.

The comparison of the galvanically active probe with the galvanically non-active reference probe show that diffusion contributes significantly to ion transport, especially to the transport of chloride ions:

The immobilization of chloride as Simonkolleit near the embedded zinc-anode creates a concentration gradient that induces chloride diffusion from the concrete cover towards the zinc-anode. Results indicate that the diffusion contributes at least 50% to the chloride transport towards the embedded zinc-anode. The alignment of the transport of chloride ions by diffusion and migration, allows significant chloride extraction of the concrete cover despite the weak electric field generated by the galvanic element zinc – iron. Furthermore, chloride is immobilized in the zinc-embedding binder matrix as Simonkolleit.

Therefore, galvanic chloride extraction and immobilization in the embedding matrix is slow. It may lead, over the service time of an embedded galvanic zinc anode (15 – 35 years depending on zinc load and average current), to significant reduction of chloride levels in the phase boundary steel-concrete up to several mm surrounding reinforcement.

There remain open questions that have to and will be dealt with:

- The definitive identification of the mineral phases and their chemical composition of the zinc-compounds in which chloride is bound are important and are underway and will be reported.
- The reasons for the very low concentration of chloride in the binder matrix will be evaluated. The diffusion constant of chloride in the embedding binder matrix will be determined.

5. References

1. J.L. Kepler, D. Darwin and J.R. Locke, *Evaluation of Corrosion Protection Methods for Reinforced Concrete Highway Structures*, Structural Engineering and Engineering Materials SM Report No. 58, University of Kansas Center for Research Inc., Lawrence, Kansas, May 2000
2. Y. P. Virmany, G.G. Clemena, *Corrosion Protection-Concrete Bridges*, Report No. FHWA-RD-98-088, Federal Highway Administration, Washington, D.C., 1998
3. R.J. Kessler, R.G. Powers, and I.R. Lasa, *Un update on the long-term use of cathodic protection of marine*

structures, Corrosion 2002, paper 02254, NACE International

4. S. Szabo, I. Bakos, *Cathodic Protection with Sacrificial Anodes*, Corrosion Reviews 24: 2006, pp. 231 – 280
5. S.J. Bullard, S. Cramer and B.Covino, *Final Report – Effectiveness of Cathodic Protection*, SPR 345. Report No. FHWA-OR-RD-09-18, National Energy Technology Laboratory, Oregon, 2009
6. W. Schwarz, A. Pichlhöfer, A. van den Hondel and H. Esteves, *Maintenance and repair of steel reinforced concrete structures by galvanic corrosion protection – field experiences over 10 years, ICCRRR 2018 Cape Town, South Africa, November 19-21, 2018, in* MATEC Web of Conferences 199, 05005 (2018)
7. W. Schwarz, F. Müllner, A.J. van den Hondel, *Maintenance and repair of steel reinforced concrete structures by simultaneous galvanic corrosion protection and chloride extraction, fib Symposium 2016, Cape Town, South Africa 21-23 November 2016*
8. A. Delagrave, J. Marchaud, and E. Samson, *Prediction of Diffusion Coefficients in Cement-Based Materials on The Basis of Migration Experiments*, Cement and Concrete Research, Vol. 26, No. 12, pp. 1831-1842, 1996
9. C. Andrade, Calculation of chloride diffusion coefficients in concrete from ionic migration measurements, Cement and Concrete Research, Volume 23, Issue 3, May 1993, Pages 724-742
10. L. Tang, H. E. Sørensen, *Precision of the Nordic test methods for measuring the chloride diffusion/migration coefficients of concrete*, Materials and Structures, Vol. 34, October 2001, pp 479-485
11. B. Elsener, U. Angst, *Mechanism of electrochemical chloride removal*, Corrosion Science, Volume 49, Issue 12, December 2007, 4504-4522
12. "Cathodic Protection of Steel in Concrete, ISO EN 12696 (2012 IDT)
13. E. Samson, J. Marchand, K.A. Snyder, Calculation of ionic diffusion coefficients on the basis of migration test results, Materials and Structures, Vol 36, April 2003, pp 156 – 165
14. W. Schwarz, F. Müllner, A. van den Hondel, "Maintenance and repair of reinforced concrete structures by simulatanous galvanic corrosion protection and chlorid extraction – field experience" fib Symposium 2016, Cape Town, South Africa 21 – 23 November 2016
15. W. Schwarz, Gerd Wilsch, A. Pichlhöfer, G. Ebell, T. Völker, „Galvanic chloride extraction by an embedded zinc anode: Ion distribution mapped by laser induced breakdown spectroscopy (LIBS)" Concrete Solutions 7th International Conference on Concrete Repair, Cluj Napoca, Romania, 30 Sep to 2 Oct 2019
16. Cremers, D.; Radzemski, L., 2006: *Handbook of Laser-induced Breakdown Spectroscopy*, John Wiley & Sons Ltd (2006).
17. G. Wilsch, F. Weritz, D. Schaurich, H. Wiggenhauser, *Determination of chloride content in concrete structures with laser-induced breakdown spectroscopy*, Construction and Building Materials 19 (10) (2005) 724 – 730. doi:10.1016/j.conbuildmat.2005.06.001.
18. G. Wilsch, D. Schaurich, H. Wiggenhauser, *Imaging laser analysis of building materials - practical examples*, AIP Conference Proceedings 1335 (1) (2011) 1315 – 1322. doi:10.1063/1.3592085.
19. G. Wilsch, T. Eichler, S. Millar and D. Schaurich, *Laser Induced Breakdown Spectroscopy (LIBS) - alternative to wet chemistry and micro-XRF*, CRC Press 2014 (2014) 611 – 615. doi:10.1201/b17394-94
20. S. Millar, C. Gottlieb, T. Guenther, N. Sankat, G. Wilsch, S. Kruschwitz, *Chlorine deter-mination in cement-bound materials with Laser-induced Breakdown Spectroscopy (LIBS) - A review and validation*, Spectrochimica Acta Part B: Atomic Spectroscopy, Volume 147, September 2018, p. 1-8
21. S. Cousy, N. Gorodylova, L. Svoboda, J. Zelenka, "Influence of synthesis conditions over simonkolleite/ZnO precipitation", Materials Science, Chemistry, Chemical Papers, (Published 15 June 2017)
22. E. Yogarajah, T. Nawa, K. Kurumisawa, "Electrokinetic potential of hydrated cement in relation to adsorption of chlorides", Cement and Concrete Research 39(4):340-344, (2009)